ภาคผนวก ก

การเผยแพร่ผลงานวิจัย

บทความที่ 1

International Conference on Electrical Engineering/Eletronics, Computer, Telecommunications and Information Technology 2013 15-17 May 2013 at Maritime Park and Spa resort Krabi

A PWM Technique to Minimize Torque Ripple in BLDC Motor for Low-Cost Applications

Srivichai Promthong
Department of Electrical Engineering
King Mongkut's University of Technology Thonburi
Bangkok, Thailand
E-mail:chaip764@gmail.com

Mongkol Konghirun
Department of Electrical Engineering
King Mongkut's University of Technology Thonburi
Bangkok, Thailand
E-mail:mongkol.kon@kmutt.ac.th

***Abstract*— This paper proposes a pulse-width modulation (PWM) technique for minimizing the torque ripple in BLDC motor. To reduce the torque ripple, the commutation interval time should be firstly known. The conventional methods of torque ripple reduction require parameters and commutation interval time computation which is sensitive to parameter variation. The proposed method is robust because the commutation interval time is mainly determined by measured terminal phase voltages. It is also low-cost scheme with minimum number of devices and not sensitive to motor parameters. The purposed method primarily computes the optimal duty ratio applied during commutation intervals to minimize the torque ripple. Both simulation and experimental results are presented to validate the proposed method, comparing with the conventional method.**

Keywords*— *Brushless dc motor; commutation interval time; current ripple reduction; torque ripple

I. INTRODUCTION

Nowadays, the energy saving is essential because of the rising energy price and global warming issues. Brushless dc (BLDC) motors have been widely applied in industry and home application for energy saving concerns. Such applications are air conditioner, refrigerator, washing machine and etc. In these applications, the vibration is undesirable effect in the system. Torque ripple produced in BLDC motor drive system causes oscillating motor speed and resonance in mechanical portions of the drive, leading to acoustic noises and observable vibration in high-precision machines. Thus, the torque ripple produced by the motors should be minimized. The BLDC motor typically is driven based on commutation of every 60 electrical degrees. The torque ripple of this conventional method is highly generated because during commutation intervals the motor current naturally flows through the freewheeling diodes [1]. In literatures, the minimization of torque ripple could be accomplished by dc bus voltage control method. However, the additional dc link voltage control circuits are required, increasing overall cost [2]-[3]. Another method of torque ripple reduction is current control method. The method is based on a strategy in which the current slopes of incoming and outgoing phases during commutation intervals can be equalized by proper duty ratio control [4]. However, this method also requires the current sensors, increasing overall cost. In [5], the wide angle control method of reducing torque ripple by means of driving the quasi-sinusoidal current was proposed. Their results showed that torque ripple in sinusoidal current drive is better than square drive control. Unfortunately, the phase current is delayed in high speed range due to the winding dynamics and back EMF. Therefore, this might introduce the higher torque ripple in high speed range. In [6], the torque ripple is reduced by changing switching sequence from 120° to 180° conduction mode at high speed because of phase commutation decrease to lower than of 120° conduction mode. However, the commutation interval time is determined by calculations which require the calculations time and higher performance MCU's. In [7], a novel PWM technique for torque ripple reduction was proposed. The calculation of commutation interval time for this PWM technique is required. Unfortunately, this calculation is complicated and sensitive to parameter motor variation. In [8], the effective commutation torque ripple using difference PWM modes was presented. The results showed that the PWM-ON pattern achieves the smallest torque ripple. The proposed PWM technique in [9] has been designed to use the detection circuits for determining the commutation inverter time without software computation. However, this method must use six op-amp comparator circuits. Therefore, this might increase overall cost as well.

In this paper, the PWM technique is therefore proposed to minimize the torque ripple and designed to overcome the disadvantages from other torque ripple reduction methods. Adjustment of duty cycle during commutation intervals can minimize the torque ripple. The incoming and outgoing phase currents are properly shaped such that the resulting phase current ripple is minimized during commutation intervals.

Moreover, only terminal phase voltages are measured for calculating the commutation interval time. In addition, the fewer number of devices is used with less computation. Consequently, this proposed method is suitable to the low-cost applications. Effectiveness of proposed method is verified by using PSIM simulations and experiments with the 200W BLDC motor.

II. Analysis of Torque Ripple during Commutation Interval Time

Theoretically, the BLDC motor produces the trapezoidal back-EMF waveform and the waveform of the excited phase current is quasi square shape as shown in Fig. 1. The three phase voltage equations can be expressed in equation (1) [1].

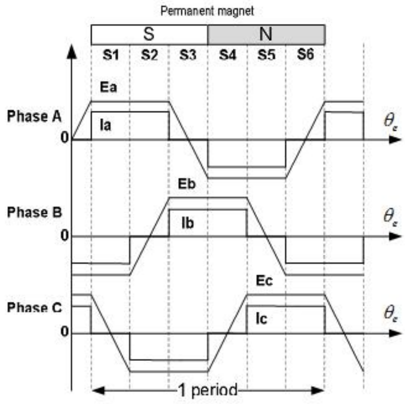

Fig. 1. Waveforms of ideal phase currents and back EMFs

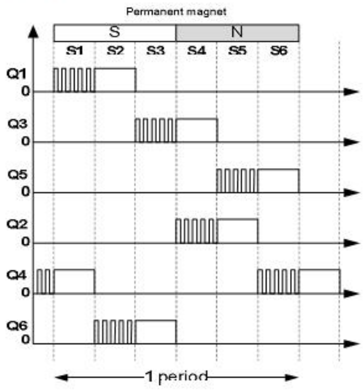

Fig. 2. Switching pattern of conventional PWM-ON technique

$$\begin{bmatrix} v_{an} \\ v_{bn} \\ v_{cn} \end{bmatrix} = \begin{bmatrix} R & 0 & 0 \\ 0 & R & 0 \\ 0 & 0 & R \end{bmatrix} \begin{bmatrix} i_a \\ i_b \\ i_c \end{bmatrix} + \begin{bmatrix} L & 0 & 0 \\ 0 & L & 0 \\ 0 & 0 & L \end{bmatrix} \frac{d}{dt} \begin{bmatrix} i_a \\ i_b \\ i_c \end{bmatrix} + \begin{bmatrix} E_a \\ E_b \\ E_c \end{bmatrix} \quad (1)$$

Electromagnetic torque can be found by equation (2).

$$T_e = \frac{1}{\omega_m}\left(E_a i_a + E_b i_b + E_c i_c\right) \quad (2)$$

Where R, $L = L_s - M$, L_s and M are resistance, self-inductance and mutual inductance, respectively.

v_{an}, v_{bn}, v_{cn} are the phase voltages of stator windings;

i_a, i_b, i_c are the phase currents of stator windings;

E_a, E_b, E_c are the phase back EMFs;

ω_m is the mechanical angular velocity of BLDC motor;

T_e is the electromagnetic torque;

Fig. 2 shows the switching pattern of conventional PWM-ON technique, consisting of six stages (S1, S2, … and S6). The upper IGBT switches of phase-a, -b, and -c (Q1, Q3, and Q5) are shopped in one-sixth of fundamental period before the following 60° electrical degrees these switches are always turned on. For the lower IGBT switches of phase-a, b, and c (Q2, Q4, and Q6), they are similarly operated as the upper IGBT switches. In each phase, the upper and lower IGBT switches are operated with phase difference of 180° electrical degrees.

Fig. 3 illustrates the commutations of the phase currents from phase-a to phase-b between stages S2 and S3. The current flowing is mainly performed by switching-off Q1 and switching-on Q3. In reality, the phase current does not immediately commute. The freewheeling diode of Q2 will provide the current path during this commutation interval until the phase-a current reduces to zero as seen in Fig. 3 (b). Finally, the phase-b current would flow through switches Q3 and Q6 in the stage S3 as show in Fig. 3 (c).

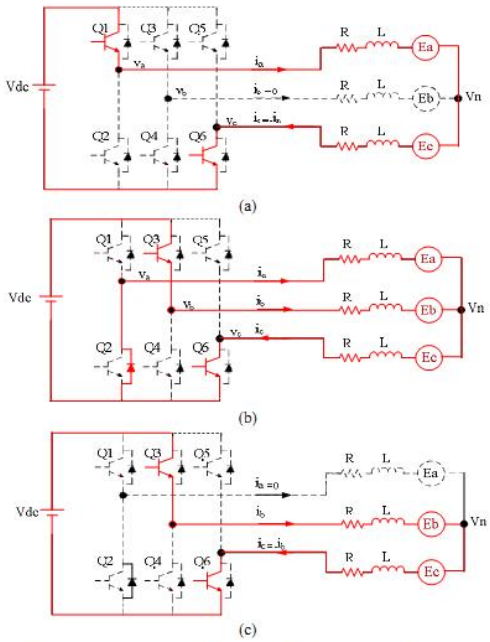

Fig. 3. Phase current commutation from phase-a to phase-b (a) Phase-a current conduction (b) During commutation interval time. (c) Phase-b current conduction

Referring to the current commutation from phase-a to -b in Fig.3 (b), the phase voltage equations can be derived by Kirchhoff's voltage law as follows.

$$V_a = 0 = R.i_a + L.\frac{di_a}{dt} + E_a + V_n \quad (3)$$

$$V_b = S_b.Vdc = R.i_b + L.\frac{di_b}{dt} + E_b + V_n \quad (4)$$

$$V_c = 0 = R.i_c + L.\frac{di_c}{dt} + E_c + V_n \quad (5)$$

$$V_n = \frac{1}{3}\left[Vdc.S_b - \left(E_a + E_b + E_c\right)\right] \quad (6)$$

where Vdc and S_b are dc-bus voltage and the switch function of Q3, respectively. When S_b = 1 meaning that Q3 is turn on and S_b = 0 meaning that Q3 is turn off.

During commutation interval time shown in Fig. 3, the phase current is commutated from phase-a to -b. The back EMF is now $E_a = E_b = -E_c = E = K_e\omega_m$. According to the Kirchoff's current law, $i_a + i_b + i_c = 0$. Therefore, electromagnetic torque in equation (2) can be rewritten as

$$T_e = \frac{-2Ei_c}{\omega_m} = -2K_e i_c \quad (7)$$

where K_e and E are back EMF constant and peak value of back EMF, respectively.

During the commutation interval time, the phase-a, -b, and -c currents are considered in three different cases. Firstly, when the phase-a current is decaying with the same rate of the rising time of phase-b current, the phase-c current and torque are constant as seen in Fig. 4(a). These are desirable current and torque waveforms. In the second case, when the phase-a current decays faster than the rising time of phase-b current, therefore the phase-c current and torque are decreased as shown in Fig. 4(b). Thirdly, the phase-a current decays slower than the rising time of phase-b current. As a result, the phase-c current and torque are increased as seen in Fig. 4(c).

As seen in this Fig. 4, and equation (7), the pulsating phase currents can cause the torque ripple during commutation interval time.

III. Proposed PWM Technique minimizing torque ripple

Fig. 5 shows the configuration circuits of inverter and BLDC motor drive system. The rotor position is detected by Hall sensors (Ha, Hb, and Hc). The upper IGBT switches (Q1, Q3, and Q5) and lower IGBT switches (Q2, Q4, and Q6) are operated in PWM-ON technique. Three terminal phase voltages are measured in the system using differential amplifiers. The commutation interval time can be directly determined by these measured terminal phase voltage signals as shown in Fig. 6. Next subsection will explain the determination of commutation inverter time.

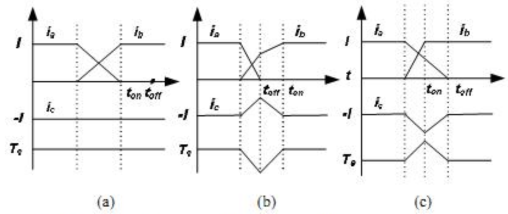

Fig. 4. Phase current and torque during commutation from phase-a to b (a) desired current and torque (b) current and torque in case of $|di_a/dt|>|di_b/dt|$, and (c) current and torque in case of $|di_a/dt|<|di_b/dt|$

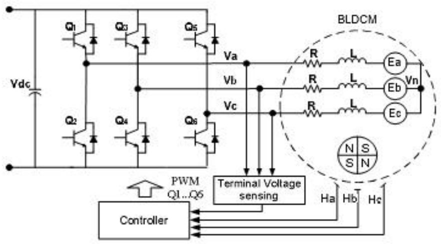

Fig. 5. Configuration circuits of inverter and BLDC motor drive system

A. Determination of commutation interval time

The proposed method primarily determines the commutation interval time based on measured three terminal phase voltages (Van, Vbn, and Vcn). When considering the terminal phase-a voltage, two commutation points can be detected as shown in Fig. 6. In case of rising edge the terminal voltage of floating phase, the commutation interval occurred before the terminal voltage is floating. Terminal phase voltage during the commutation time is equal to dc bus voltage. On the other hands, in the case of falling edge the terminal voltage of floating phase, the commutation interval occurred before the terminal voltage is floating. However, terminal phase voltage during the commutation time is equal to zero voltage. Finally, the determination of commutation interval time in every stage is summarized in Table I.

TABLE I
COMMUTATION PERIOD DETECTION

Stage	Commutation period detection
S1	Terminal voltage phase-c, V_{cn}= 0
S2	Terminal voltage phase-b, V_{bn}= Vdc
S3	Terminal voltage phase-a, V_{an}=0
S4	Terminal voltage phase-c, V_{cn}= Vdc
S5	Terminal voltage phase-b, V_{bn}=0
S6	Terminal voltage phase-a, V_{an}=Vdc

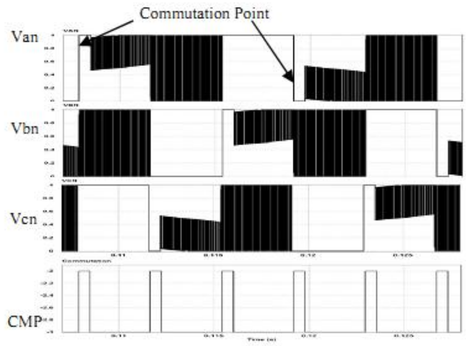

Fig. 6. Terminal phase voltages and commutation interval time

B. *Proposed PWM technique*

In Fig. 7, the switching pattern of proposed PWM technique is shown. As seen, six additional commutation intervals are inserted between 60 electrical degrees. To minimize torque and current ripples, the duty cycle is optimally calculated during commutation intervals. Referring to equation (6), the duty cycle during commutation interval time can be represented as follows [10].

$$D_{cmp} = \frac{3}{2}D + \frac{K_e \omega_m}{Vdc} \quad (8)$$

where D and D_{cmp} are duty cycle during non-commutation and duty cycle during commutation, respectively.

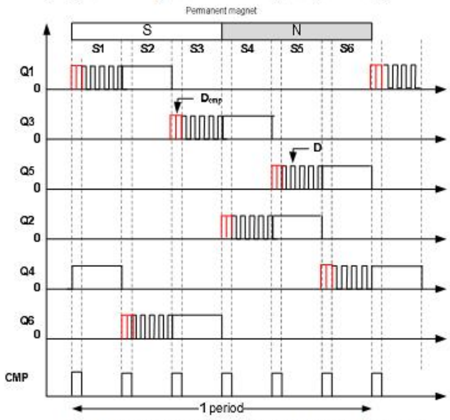

Fig. 7. Switching pattern of proposed PWM technique

IV. Simulation Results

To verify the proposed method, the PSIM program version 9.0.3.400 is employed. The parameters of BLDC motor used in simulation and experiment are summarized in Table II. Fig. 8 shows the overall block diagram of proposed system using PSIM simulator. The controller block is written by C language, and it is compiled into DLL and link it in PSIM program. Thus, the same C codes can be directly ported into the real controller.

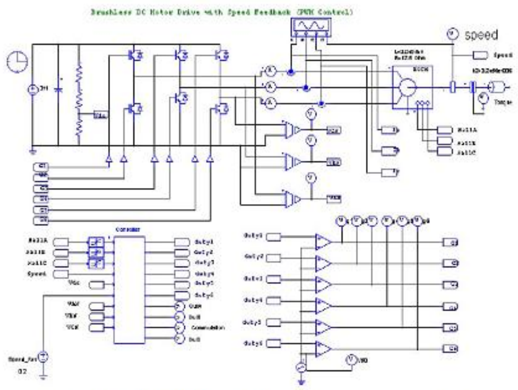

Fig. 8.Overall PSIM block diagram of the proposed system

TABLE II
BLDC Motor parameters

No. of poles	4
DC link voltage	311 V
Rated power	200 W
Resistance	12.5 Ω
Inductance	45 mH
Back EMF constant	0.0323 v/rpm

Fig. 9 shows the simulated waveforms of phase currents commutation intervals and PWM signals of Q3 and Q6 in case of the conventional PWM-ON technique previously presented in Fig. 2. In this simulation, the motor speed is 2,000 rpm. In Fig. 9(b), it is clearly that the decaying rate of phase-a current and the rising rate of phase-b current are not equal to each other. Therefore, the phase-c current has ripple. Fig. 9(c) shows the PWM signals of Q3 during current commutation from phase-a to phase-b without adjusting the duty cycle.

Next, the same overall block diagram of BLDC motor drive with the same speed condition of 2,000 rpm is tested with the proposed PWM-ON technique. Fig. 10 shows the simulated waveforms of phase currents commutation intervals and PWM signals of Q3 and Q6 in case of the proposed PWM technique shown in Fig. 7. As expected, the major improvement of current ripple can be observed in Fig. 10(a). In Fig. 10(b), the decaying rate of phase-a current and the rising rate of phase-b current are equal to each other, resulting in the smooth phase-c current without ripple. The PWM signals of Q3 during current commutation from phase-a to phase-b with adjusting the duty cycle can be seen in Fig. 10(c).

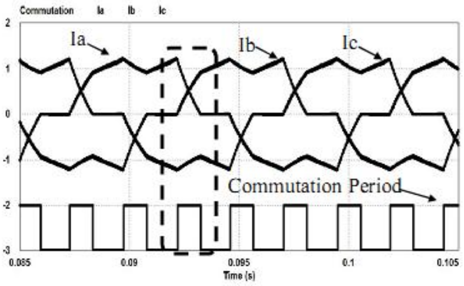

(a)

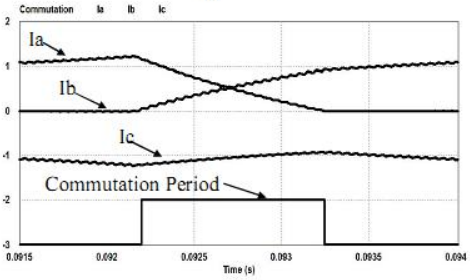

(b)

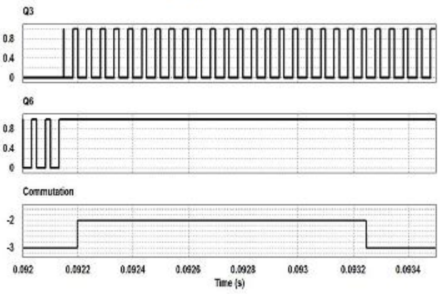

(c)

Fig. 9. Simulation results of the conventional method at 2,000 rpm (a) phase currents and commutation intervals (b) zoomed waveforms in the dotted box shown in (a), and (c) PWM signals of Q3 and Q6 during current commutation from phase-a to phase-b

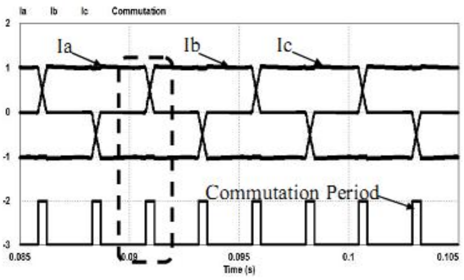

(a)

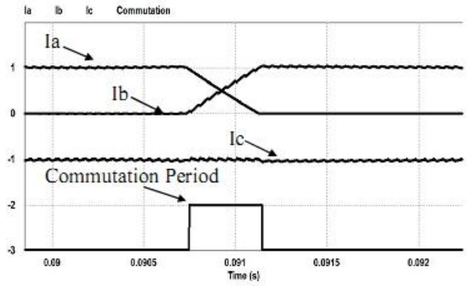

(b)

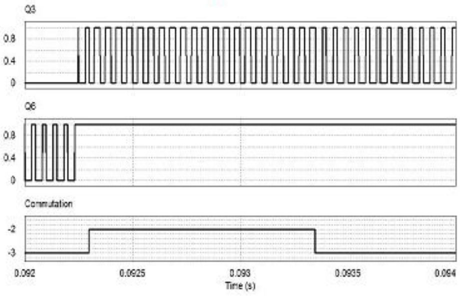

(c)

Fig. 10. Simulation results of the proposed method at 2,000 rpm (a) phase currents and commutation intervals (b) zoomed waveforms in the dotted box shown in (a), and (c) PWM signals of Q3 and Q6 during current commutation from phase-a to phase-b

V. EXPERIMENTAL RESULTS

In experiments, a fixed-point, 16-bit, 40 MIPS dsPIC33F controller is used to implement the proposed method. The switching frequency of the inverter is 16 kHz. The dc-bus voltage is 310 volt. The motor shaft is connected to a fan's dummy load. The setup of BLDC motor drive system is shown in Fig. 11.

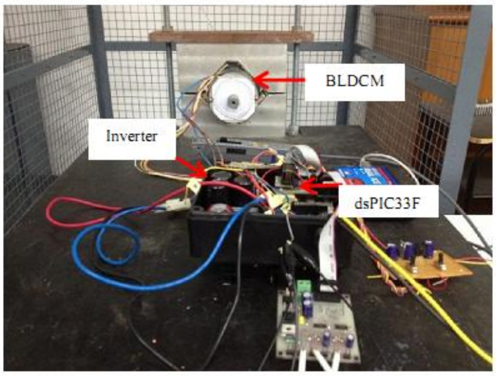

Fig. 11. Setup of BLDC motor drive system

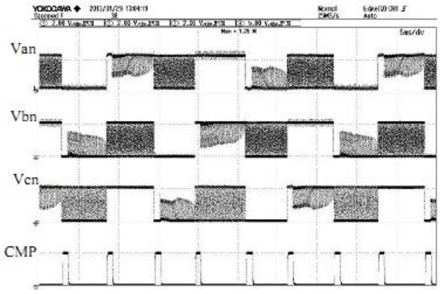

Fig. 12. Experimental results of output signal terminal phase voltages sensing and commutation intervals (2V/div, 5 ms/div)

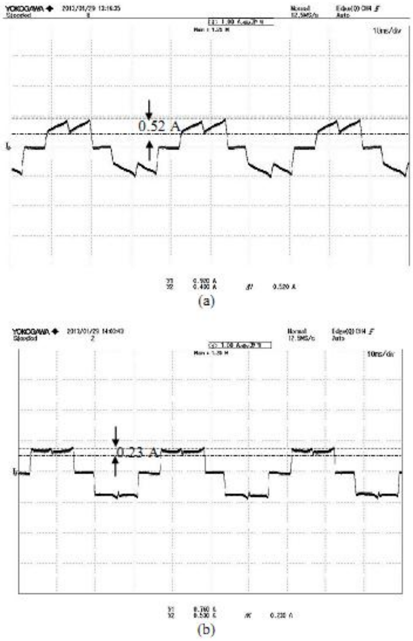

Fig. 13. Experimental results of phase-c current at 900 rpm (1A/div, 10 ms/div). (a) conventional method, and (b) proposed method

Fig. 12 shows the measured output signal of terminal phase voltages sensing and commutation intervals based on the measurement of terminal phase voltages, as previously explained in Fig. 6.

Fig. 13 shows the experimental results of phase-c current at motor speed 900 rpm for both conventional and proposed methods. Obviously, the current ripple can be reduced from 0.52 A to 0.23A or 55.7% reduction when using the proposed PWM technique.

VI. Conclusions

This paper presented a PWM technique to minimize torque ripple in BLDC motor for low-cost applications. The proposed method directly uses the measured terminal phase voltages to determine the commutation intervals. It is cost effective PWM technique for further development of sensorless BLDC motor drive. However, this proposed method has been designed for low and medium speed ranges. In high speed region or high load, the compensated duty cycle will be limited. Thus, the weaker suppression of torque ripple during commutation is expected. According to both simulation and experimental results, the effectiveness of proposed method has shown, significantly minimizing the torque and current ripples.

Acknowledgment

This work was supported by the Higher Education Research Promotion and National Research University Project of Thailand, Office of the Higher Education Commission.

References

[1] R. Carlson, M. Lajoie-Mazenc, and J. C. D. S. Fagundes, "Analysis of torque ripple due to phase commutation in brushless DC machines," IEEE Transactions on Industry Applications, vol. 28, 632-638, 1992.

[2] N. Ki-Yong, et al., "Reducing torque ripple of brushless DC motor by varying input voltage," IEEE Transactions on Magnetics, vol. 42, 1307-1310, 2006.

[3] J. Jin-soek and K. Byung-taek, "Minimization of torque ripple in a BLDC motor using an improved DC link voltage control method," in Telecommunications Energy Conference, 2009.

[4] S. Joong-Ho and C. Ick, "Commutation torque ripple reduction in brushless DC motor drives using a single DC current sensor," in IEEE Trans. on Power Electronics, vol. 19, 312-319, 2004.

[5] C. H. Wu, et al., "A wide-angle wave control method of reducing torque ripple for brushless DC motor," Journal of Shanghai University, vol. 11,pp. 300-303, 2007.

[6] S.S. Bharatkar, et al., " Dual-mode switching technique for reduction of commutation torque ripple of brushless dc motor," Journal of IET Electric Power Applications, vol. 5, 193-202, 2011.

[7] S. S. Bharatkar, R. Yanamshetti, D. Chatterjee, and A. K. Ganguli, "Reduction of commutation torque ripple in a brushless dc motor drive," in Proc. IEEE PECon, 2008.

[8] H.S. Chuang, Yu-Lung Ke, and Y.C. Chuang, "Analysis of commutation torque ripple using different PWM modes in BLDC motors," in Proc. IEEE ICPS, 2009.

[9] Yong-Kai Lin and Yen-Shin Lai, "Pulse-width modulation technique for BLDCM drives to reduce commutation torque ripple without calculation of commutation time," IEEE Transactions on Industry Applications, vol. 47, pp. 1786-1793, 2011.

[10] Dae-Kong Kim, et al., "Commutation torque ripple reduction in a position sensorless brushless DC motor drive," in IEEE Trans. on Power Electronics, vol. 21, 1762-1768, 2006.

บทความที่ 2

International Conference on Electrical Machines and Systems 2013 26-29 October 2013

at Haeundae Grand Hotel Busan

2013 International Conference on Electrical Machines and Systems, Oct. 26-29, 2013, Busan, Korea

Sensorless control of BLDC motor drive with 150° conducting mode to minimize torque ripple

Srivichai Promthong and Mongkol Konghirun
Department of Electrical Engineering, King Mongkut's University of Technology Thonburi, Thailand
E-mail: chaip764@gmail.com and mongkol.kon@kmutt.ac.th

Abstract — This paper presents the sensorless control of BLDC motor drive with 150° conducting mode for minimizing the torque ripple. The proposed method defines the energizing interval in phase voltage commutation every 30 electrical degrees. In each phase commutation, two or three switches conduct alternately in order to obtain the quasi sinusoidal phase voltage waveform. Compared with traditional control, the torque ripple of BLDC motor can be significantly reduced by using the proposed method. Both simulation and experimental results have been presented to validate the reduction of torque ripple by using the proposed method.

I. INSTRODUCTION

Recently, the brushless dc (BLDC) motor is widely used in industrial applications and home appliances due to its high efficiency, high power density and low maintenance. However, the BLDC motor drive requires a position sensor which reduces the reliability of overall system. Also, the BLDC motor drive produces the torque pulsation. Torque pulsation produced in the conventional BLDC motor drive system causes the oscillating speed and resonance in mechanical portions of the drive, leading to acoustic noises and observable vibration in machines. Since an ideal BLDC motor theoretically has a trapezoidal back-EMF waveform, the BLDC motor has to be fed by an ideal rectangular current waveform. In practice, the BLDC motor drive inherently produces the current ripple during commutations because the motor current naturally flows through the freewheeling diodes [1]. To improve the torque ripple, the methods in [2]-[3] proposed the novel PWM to eliminate the ripple current by using PWM_ON_PWM mode. However, the commutation interval time is determined by calculations which require the computation time and higher performance MCU's. In [4], the effective commutation torque ripple using different PWM modes was presented. The results showed that the PWM-ON pattern achieves the smallest torque ripple. Another method of torque ripple reduction in a sensorless BLDC motor drive was proposed in [5]. Their proposed method used the measured terminal phase voltages to determine the commutation intervals and then computed the optimal duty ratio applied during commutation intervals to minimize the torque ripple. However, it did not provide the good performance in high speed operation because of limitation of duty cycle compensation.

Although the fed current could be typically controlled as rectangular waveform, the torque ripple is still produced due to the non-ideal back EMF. The ideal back EMF would be trapezoidal shape. There are many reasons of non-ideal back EMF in the BLDC motor such as non-uniformity of magnetic material, stator winding configuration, tooth winding with pole shoe, and etc. as shown in Fig.1 [6].

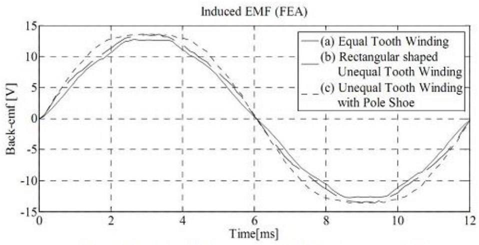

Fig.1 Comparative FEA back EMF's waveforms [6]

In order to reduce the torque ripple in BLDC motor with non-ideal back EMF, In [7], the new current control method was adopted. The duty cycle was calculated in the current controller by measuring the angular position and the offline measured back EMF. This method could reduce the torque ripple in both low and high speeds. However, this method required the position sensor, increasing the overall cost, reliability and complexity because of the offline measured back EMF. The methods in [8]-[9] showed that the sinusoidal current drive could reduce the torque fluctuation better than square drive control. However, these methods needed the position sensors, current sensor and increased switching losses, comparing with traditional control drive system.

In this paper, the wide angle control commutation technique is proposed to minimize the torque ripple in the sensorless BLDC motor drive. Instead of square current drive control, the sinusoidal current is driven into the trapezoidal back EMF. In order to obtain phase current quasi sinusoidal waveform, the commutations of every 30 electrical degrees are needed. Therefore, there are twelve states in each electrical period. During each conduction interval, two or three switches are alternately conducted and each phase winding is conducted by 150°. In addition, the terminal phase voltages sensed by voltage sensors are used for computing the commutation states

978-1-4799-1447-0/13/$31.00 ©2013 IEEE

by means of zero crossing detection of back EMF [10]-[11]. Effectiveness of proposed method is verified by PSIM simulation and experimentation with a 200W BLDC motor.

II. Analysis of Torque Ripple for Conventional 120^o Conducting Mode

Theoretically, the BLDC motor produces the trapezoidal back-EMF waveform and the waveform of the excited phase current is quasi square shape as shown in Fig. 2. However, in practical, the currents does not commutate instantaneously due to the effect of stator winding inductance and freewheeling diode [1],[12] as shown in Fig.3. This leads to high torque ripple in BLDC motor.

The BLDC motor drive has two operation regions; conduction and commutation regions as illustrated in Fig.3. In the conduction region, only two phase windings (phase-a and c) are conducted for 120^o according to the rotor electrical position while the phase-b winding is inactive. In the commutation region, the previously inactive phase-b winding would be energized. During this region, the phase-a will be switched off, the phase-b will be switched on and the phase-c will remain conducting. Both conduction and commutation regions operate in six states in each electrical period. In order to analyze the torque ripple, the electromagnetic torque equation is simply shown in (1).

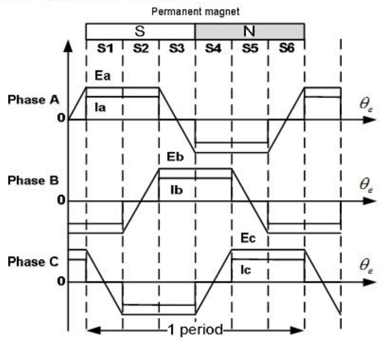

Fig. 2. Waveforms of ideal phase currents and back EMFs

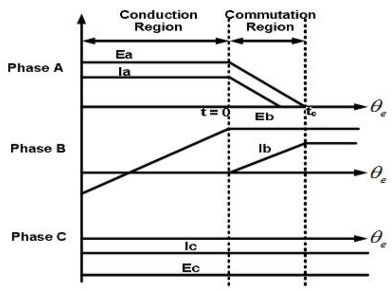

Fig. 3. Waveforms of practical phase currents and back EMFs in conduction and commutation regions

$$T_e = \frac{1}{\omega_m}\left(E_a i_a + E_b i_b + E_c i_c\right) \tag{1}$$

where T_e is the electromagnetic torque, i_a, i_b, i_c are the phase currents of stator windings, E_a, E_b, E_c are the phase back EMFs and ω_m is the mechanical angular velocity of BLDC motor.

To evaluate the proposed drive performance, the percentage of torque ripple in a BLDC motor is defined as:

$$\%T_{ripple} = \frac{\Delta T_{peak-peak}}{T_{avg}} x100\% \tag{2}$$

where $\%T_{ripple}$ is the percentage of torque ripple, $\Delta T_{peak-peak}$ is the peak-to-peak torque and T_{avg} is the average torque.

A. Torque ripple in conduction region

Referring to Fig. 3, to analyze the torque ripple in conduction region, the phase currents and back EMFs in state S2 in Fig. 2 are considered. Two conducting phase currents consist of phase-a and phase-c while the non-conducting phase is phase-b. Therefore, both switches associated with phase-b winding would be turned off. Three phase current in state S2 can be described as follows.

$$i_a = I_o, i_b = 0, \text{and } i_c = -I_o \tag{3}$$

Moreover, the phase back EMF in state S2 can be expressed as

$$E_a = E, E_b = \frac{6E}{\pi}\theta + E \text{ and } E_c = -E \tag{4}$$

Substituting (3) and (4) into (1), the electromagnetic torque can be rewritten as

$$T_e = \frac{1}{\omega_m}\left(E\,.I_o + E_b.0 + (-E).(-I_o)\right) = \frac{2EI_o}{\omega_m} \tag{5}$$

where I_o, E and θ are the peak value of current, peak value of back EMF and rotor position, respectively.

According to (5), the pulsation of phase conducting currents primarily leads to the torque ripple in conduction region.

B. Torque ripple in commutation region

Referring to Fig. 3, the commutation of the phase currents from phase-a to phase-b between states S2 and S3. In practice, the phase currents does not commutate instantaneously due to the effect of stator winding inductance and freewheeling diode. Three phase current in this region can be expressed as

$$i_a = I_o - \frac{I_o}{t_c}\theta, i_b = \frac{I_o}{t_c}\theta, \text{and } i_c = -I_o \tag{6}$$

The phase back EMF in the commutation stage between state S2 and S3 can be derived as

$$E_a = \frac{6E}{\pi}\theta + E, E_b = E \text{ and } E_c = -E \quad (7)$$

Substituting (6) and (7) into (1), the electromagnetic torque during this commutation region can be rewritten as

$$T_e = \frac{1}{\omega_m}\left(\frac{6E}{\pi}\theta + E.(I_o - \frac{I_o}{t_c}\theta) + E_b.\frac{I_o}{t_c} + (-E).(-I_o)\right)$$

$$T_e = \frac{2EI_o}{\omega_m} + \frac{6k_e I_o}{\pi}\left(\frac{\theta^2}{t_c} - \theta\right) \quad (8)$$

where t_c and k_e are the commutation interval time and the back EMF constant, respectively.

Normally, the commutation interval time (t_c) is dependent on motor speed. In the low speed range, the decaying time of phase current is used as the commutation interval time because the current of the outgoing phase would reach to zero slower than the current of the incoming phase reaching to its maximum value. On the other hands, in the high speed range, the commutation interval time is determined by using the rising time of phase current instead.

Considering the electromagnetic torque in (8), the torque ripple caused by the current ripple (i.e., $\frac{2EI_o}{\omega_m}$) and the torque ripple caused by to the commutation time (i.e., $\frac{6k_e I_o}{\pi}\left(\frac{\theta^2}{t_c} - \theta\right)$) are involved in this torque equation. Although, the current ripple can be controlled constantly by using the different techniques mentioned from different literatures, the torque ripple still remains depending on the commutation time. In order to obtain the maximum torque ripple, the equation (8) is differentiated with respect to θ as expressed in (9) [12].

$$\frac{dT_e}{d\theta} = \frac{6k_e I_o}{\pi}\left(\frac{1}{t_c}2\theta - 1\right) = 0 \quad (9)$$

Therefore, the maximum torque ripple appears when θ is equal to $t_c/2$. Substituting $\theta = t_c/2$ into (8), the electromagnetic torque can be rewritten as

$$T_e = \frac{2EI_o}{\omega_m} - \frac{3k_e I_o t_c}{2\pi} \quad (10)$$

Eventually, the torque ripple in the commutation region is proportional to the phase non-commutation current and commutation interval time.

III. PROPOSED 150° CONDUCTING MODE FOR BLDC MOTOR DRIVE

Fig. 4 shows the overall block diagram of the proposed method. All upper IGBT switches (Q1, Q3 and Q5) and all lower IGBT switches (Q2, Q4, and Q6) are operated in PWM-ON mode. The rotor position estimation method that applies the means of detecting the zero crossing points (ZCPs) of back EMFs has been widely used in the sensorless BLDC motor drive systems because of its simplicity [10]-[11]. Since the zero crossing points always lead the commutation points by 30 electrical degrees, the commutation points can be calculated by using the zero crossing information. As a result, the proposed sensorless BLDC motor drive system with 150° conducting mode is practically implemented.

The proposed method defines the energizing interval of phase current commutation every 30 electrical degrees. Therefore, there are twelve states in a fundamental period. In each phase commutation, two or three switches conduct alternately in order to obtain the quasi-sinusoidal current waveform.

The switching pattern of the proposed method consists of twelve states (i.e., S1, S2, … , and S12) as illustrated in Fig. 5. In order to describe about this switching pattern, the upper IGBT switches of phase-a, -b and –c (Q1, Q3 and Q5) are begun to fully conduct in one-twelfth of fundamental period before the following 120° electrical degrees these switches are always PWM chopped. Then, theses switches are returned fully conducting again with 120° electrical degrees. Similarly, for the lower IGBT switches phase-a, -b and –c (Q2, Q4 and Q6), they are operated the same pattern as the upper IGBT switches with a phase difference of 180 electrical degrees of pattern switches of Q1, Q3 and Q5, respectively.

Focusing on PWM states, there are two differently adjustable duty ratios. The first duty ratio is governed from PI controller and this is employed when two switches are operated in that PWM state. The second duty ratio is defined in (11) where three switches are operated.

$$D_{reduce} = \frac{\sqrt{3}}{2}D \quad (11)$$

where D and $D_{reduced}$ are the duty ratio governed by PI controller and duty ratio during three-switch conduction, respectively.

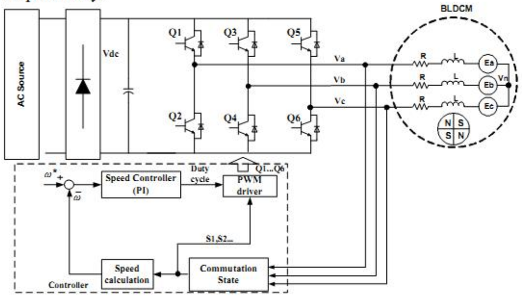

Fig. 4. Overall block diagram of proposed sensorless BLDC motor drive system.

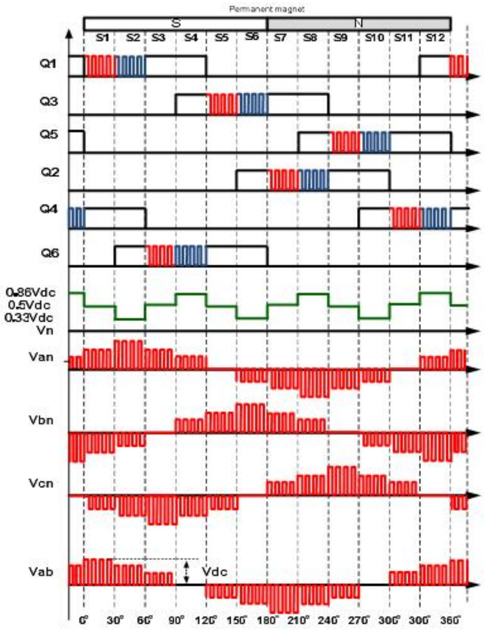

Fig. 5. Switching pattern, ideal phase voltage and line to line voltage of proposed method

Since the current and rotor position sensors do not employ in the proposed method, the current could not be perfectly controlled as sinusoidal current waveform. Fortunately, quasi-sinusoidal current waveform can be implied through the phase voltage waveform by varying the neutral point voltage (V_n) depending on switching pattern. The V_n is equal to $V_{dc}/2$ when two switches conduct. For three-switch conduction, V_n is equal to $V_{dc}/3$ (in case of one upper and two lower switches operated) or $2V_{dc}/3$ (in case of two upper and one lower switches operated) as shown in Fig.5. By adjusting V_n, the quasi-sinusoidal phase voltage can be generated. Since the proposed V_n ($V_{dc}/3$) is less than the conventional V_n ($V_{dc}/2$) when the phases current starts to rising, the torque ripple is therefore less than the conventional method.

IV. Simulation Results

To verify the proposed method, the PSIM program is employed for simulation testings. The parameters of Y-connected BLDC motor used in simulation and experiment are summarized in Table I. Fig. 6 shows the overall block diagram of proposed system using PSIM simulator. The controller block is simply written in C language, and then compiled into DLL that links to PSIM program. Thus, it is easily to port the C codes of proposed method in PSIM program to the real controller.

Fig. 7 shows the simulated terminal phase voltages based on the operation of proposed 150° conducting mode. In this Fig., as expected, these phase voltages are generated similarly to the quasi-sinusoidal waveform previously explained in Fig. 5. However, unlike the ideal phase voltages, the simulation result has slightly different due to the commutating phase current through the freewheeling diode.

In order to evaluate the torque ripple reduction, Fig. 8 and Fig. 9 show the simulated steady-state results between the conventional and the proposed method at an operating speed of 1500 rpm. Fig. 8 shows the phase current and electromagnetic torque waveforms by using conventional method. High ripple current waveforms are clearly observed in Fig. 8(a) because of the effect of freewheeling diode and large stator winding inductance. Consequently, the electromagnetic torque significantly fluctuates about 38.12% as seen in Fig. 8(b). Similarly, Fig. 9 shows the phase current and electromagnetic torque waveforms by using the proposed method. Clearly seen in Fig. 9(a), the phase current is quasi-sinusoidal waveform. Due to the effect of the quasi-sinusoidal current, the torque ripple can be lowered to 28.65%. Compared with the conventional method, the torque ripple based on the proposed PWM technique can be reduced from 38.12% to 28.65%.

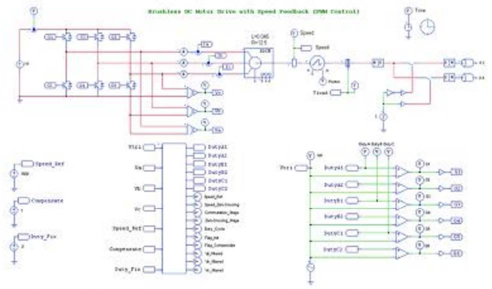

Fig. 6. Overall PSIM block diagram of the proposed system

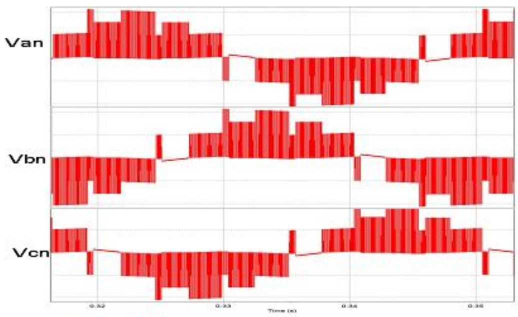

Fig. 7. Simulated terminal phase voltage of the proposed method

TABLE I
BLDC MOTOR PARAMETERS

No. of poles	4
DC link voltage	311 V
Rated power	200 W
Resistance	12.5 Ω
Inductance	45 mH
Back EMF constant , k_e	0.0323 v/rpm

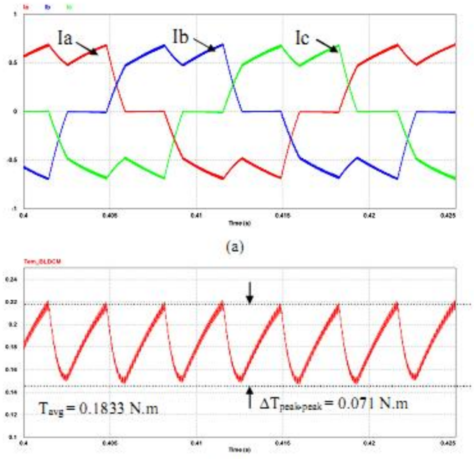

Fig. 8. Simulation results of the conventional method at 1500 rpm (a) phase currents and (b) electromagnetic torque

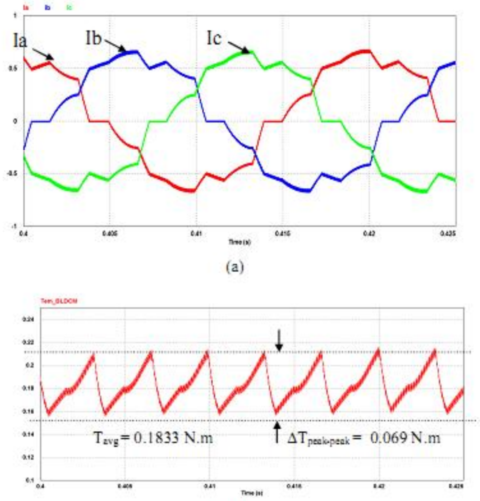

Fig. 9. Simulation results of the proposed method at 1500 rpm (a) phase currents and (b) electromagnetic torque

V. Experimental Results

In experiments, a fixed-point, 16-bit, 40 MIPS dsPIC33F controller is used to implement the proposed method compared with the conventional PWM-ON technique. The switching frequency of IGBTs is set 16 kHz. The dc-bus voltage is 310 volt. The motor shaft is connected to a fan's dummy load. A three-phase hall sensors board is already manufactured inside this particular motor. The hardware setup of BLDC motor drive system is shown in Fig. 10.

Fig. 11 shows the steady-state responses of the sensorless BLDC motor system by using the conventional method of six-step drive when motor speed is controlled at 800 rpm. During testing, three hall sensor signals (i.e., Hall A, B, and C) are not used as the system feedback but only captured for verifying the correct commutation sequences estimated by the sensorless algorithm.

Three phase voltages (i.e., Va, Vb, and Vc) are measured by using the differential amplifiers. Inactive phase voltage in each state is available to determine the zero crossing point (Zc trig signal). After the Zc trig signal is obtained, the commutation points (Cmtn trig signal) can be calculated by delaying the zero crossing point by 30 electrical degrees. These commutation points are then employed to commute the phase currents. Although the phase current state sequence correctly corresponds to the hall sensor signal sequence, the phase currents remain high ripple as shown Fig. 11.

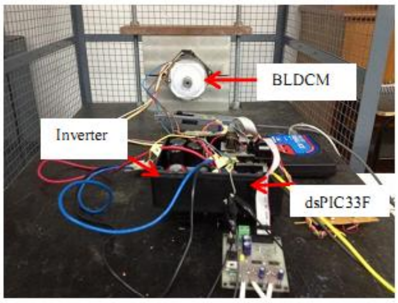

Fig. 10. Hardware setup of BLDC motor drive system

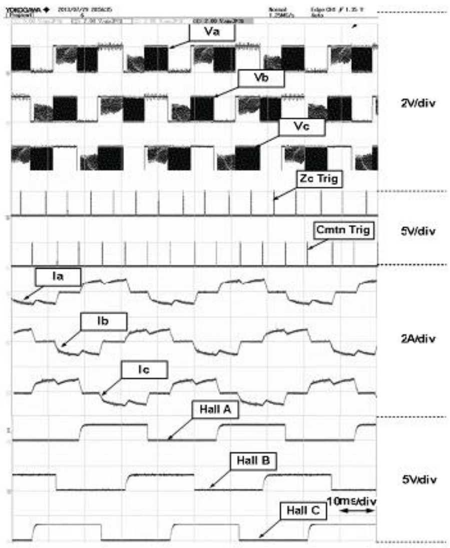

Fig. 11. Three terminal phase voltages, zero crossing points, commutation points, phase currents and three phase hall sensor signals at 800 rpm by conventional method of six-step drive

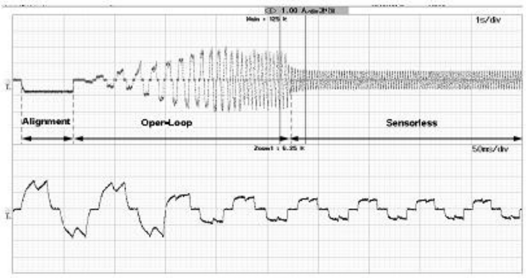

Fig. 12. Experimental results of phase-a current during starting-up

The phase-a current operating from starting-up to steady-state is shown in Fig. 12. When the power is supplied to the drive system, the controller performs three modes: (1) alignment mode, (2) open-loop starting-up mode, and (3) sensorless mode. In the first mode, the DC current feeds to the motor winding, initially locking the rotor to a known rotor position. This alignment time is 1 sec. Then, the open-loop starts up by ramping up the PWM duty cycle from 10% to 16.5% as well as the command frequency is also ramping up from 10 to 15 Hz. In this Fig., the zoomed phase current verifies that the transition from the open-loop mode to sensorless mode is smooth.

Next, Fig. 13 shows experimental result of the sensorless control of BLDC motor drive with 150° conducting mode. The phase current commutation interval is every 30 electrical degrees. With proposed switching pattern, the phase currents are shaped to the quasi-sinusoidal waveform, implying the lower torque ripple of BLDC motor.

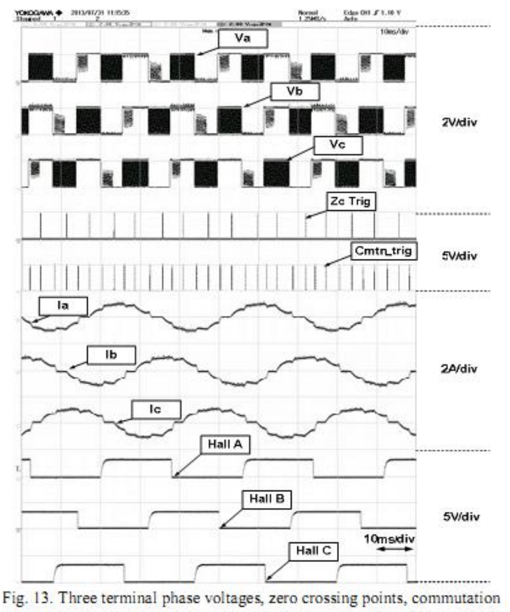

Fig. 13. Three terminal phase voltages, zero crossing points, commutation points, phase currents and three phase hall sensor signals at 800 rpm in the proposed method

VI. CONCLUSION

The sensorless control of BLDC motor drive with 150° conducting mode has been proposed and successfully implemented in this paper. The high torque ripple in the traditional 120° conducting mode for BLDC motor could be reduced when driving the BLDC motor with 150° conducting mode, generating the quasi-sinusoidal phase currents. Simulation and experimental results have been given to verify the reduction of torque ripple due to the proposed control strategy.

ACKNOWLEDGMENT

This work was supported by the Higher Education Research Promotion and National Research University Project of Thailand, Office of the Higher Education Commission.

REFERENCES

[1] R. Carlson, M. Lajoie-Mazenc, and J. C. D. S. Fagundes, "Analysis of Torque Ripple due to Phase Commutation in Brushless DC Machines," *IEEE Transactions on Industry Applications*, vol. 28, pp. 632-638, 1992.

[2] G. Meng, H. Xiong, and H. Li, "Commutation Torque Ripple in BLDC Motor Using PWM_ON_PWM Mode," in *Proc. IEEE ICEMS Conf.*, pp. 1-6, 2009.

[3] K. Wei, J. J. Ren, F. H. Teng, and Z. C. Zhang, "A Novel PWM Scheme to Eliminate the Diode Freewheeling in the Inactive Phase in BLDC Motor," in *Proc. IEEE Power Electron Conf.*, pp. 2282-2286, 2004.

[4] H.S. Chuang, Yu-Lung Ke, and Y.C. Chuang, "Analysis of Commutation Torque Ripple Using Different PWM Modes in BLDC Motors," in *Proc. IEEE ICPS Conf.*, pp. 1-6, 2009.

[5] D. K. Kim, K. W. Lee, and B. I. Kwon, "Commutation Torque Ripple Reduction in a Position Sensorless Brushless DC motor Drive," *IEEE Transactions on Power Electronics*, vol. 21, pp. 1762-1768, 2006.

[6] D. Ishak, Z.Q. Zhu and D. Howe, "Permanent Magnet Brushless Machines with Unequal Tooth Widths and Similar Slot and Pole Numbers," *IEEE Transactions on Industry Applications*, vol. 41, pp. 584-590, 2005.

[7] J. Fang, H. Li, and B. Han, "Torque Ripple Reduction in BLDC Torque Motor with Nonideal Back EMF," *IEEE Transactions on Power Electronics*, Vol. 27, pp. 4630 - 4637, November 2012.

[8] R. Ma, J. Deng, and Y. Huangfu, "A Novel Sinusoidal Current Driving Method for BLDCM Based on SVPWM," in *Proc. IEEE ICEMS Conf.*, pp. 732-735, 2010.

[9] H. J. Guo, K. Mochizuki, T. Watanabe, and O. Ichinokura "A New Control Method of BLDCM Based on Internal Model Principle," in *Proc. Int. Conf. Power Electron. Drives Syst.*, vol. 2, pp.1686 -1691, 2003.

[10] A. Ungurean, V. Coroban-Schramel, and I. Boldea, "Sensorless Control of a BLDC PM Motor Based on I-f Starting and Back-EMF Zero-Crossing Detection," *International Conference on Optimization of Electrical and Electronic Equipment*, pp. 377 – 382, May 2010.

[11] J. Shao, D. Nolan, M. Teissier, and D. Swanson, "A Novel Microcontroller-Based Sensorless Brushless DC (BLDC) Motor Drive for Automotive Fuel Pumps," *IEEE Transactions on Industry Applications*, Vol. 39, No. 6, pp. 1734 – 1740, 2003.

[12] B. Kang, C. Kim, H. Mok, and G. Choe, "Analysis of Torque Ripple in BLDC with Commutation Time," in *Proc. IEEE ISIE Conf.*, pp. 1044-1048, 2001.